 DOI: https://doi.org/10.5114/ceji/207758

CircHMGA2 facilitates proliferation and invasion of laryngeal squamous cell carcinoma cells and M2 macrophage polarization *via* the miR-384/ROCK1 axis

ZHENJUN WANG[1,2], PING WU[3], LI LI[3], XIANHUA ZHU[3#], YUEYONG XIAO[1#]

[1]Department of Radiology, the First Medical Center, Chinese PLA General Hospital, Beijing 100039, PR China
[2]Medical School, Chinese PLA General Hospital, Beijing 100039, PR China
[3]Second Affiliated Hospital of Nanchang University, Jiangxi Province, PR China
[#]*Yueyong Xiao and Xianhua Zhu are co-corresponding authors.*

Abstract

Introduction: *Laryngeal squamous cell carcinoma (LSCC) is a malignant tumor of the head and neck. CircRNA High Mobility Group AT-hook 2 (circHMGA2) has cancer-promoting functions. Nevertheless, the role of circHMGA2 in LSCC has not been reported yet. We attempted to illustrate the function and mechanism of circHMGA2 in LSCC.*

Material and methods: *The clinicopathological association between circHMGA2 and LSCC was assessed via the chi-square test. The correlation between circHMGA2 and LSCC patient survival time was determined with Kaplan-Meier analysis. Quantitative real-time PCR was applied to determine circHMGA2 expression in LSCC. Cell Counting Kit-8 assay, Western blot, cell invasion, enzyme-linked immunosorbent assay, and co-culture assays were conducted to evaluate circHMGA2 function in LSCC. Dual-luciferase reporter assay and RNA pull-down were performed to explore the role of circHMGA2 in LSCC. Meanwhile, circHMGA2 function in vivo was evaluated using tumor xenograft experiments, hematoxylin-eosin staining, and immunohistochemical assays.*

Results: *CircHMGA2 was raised in LSCC, and elevated circHMGA2 expression was associated with TNM stage of LSCC patients. Patients with elevated circHMGA2 levels had shorter overall survival. Functionally, circHMGA2 knockdown suppressed LSCC cell proliferation and invasion. Also, circHMGA2 knockdown inhibited M2 macrophage polarization. Mechanistically, circHMGA2 targeted miR-384, and miR-384 targeted ROCK1. Also, ROCK1 level was negatively associated with miR-384 in LSCC tissues, but positively associated with circHMGA2. Moreover, rescue experiments suggested that circHMGA2 knockdown ameliorated LSCC growth via miR-384/ROCK1 and suppressed M2 macrophage polarization through miR-384/ROCK1. Meanwhile, circHMGA2 knockdown inhibited LSCC growth in vivo.*

Conclusions: *CircHMGA2 acts as a competing endogenous RNA, promoting LSCC progression through the miR-384/ROCK1 axis.*

Key words: *circHMGA2, LSCC, M2 macrophage polarization, miR-384, ROCK1.*

(Cent Eur J Immunol 2026; 51:)

Introduction

Laryngeal squamous cell carcinoma (LSCC) is a common tumor of the head and neck, and its incidence and mortality continue to increase annually [1, 2]. Pathological factors of LSCC include excessive drinking and smoking [3]. Nowadays, surgery is the primary treatment for LSCC, supplemented by chemotherapy [4]. Although clinical outcomes for LSCC have been improved to some extent, the LSCC prognosis is still not optimistic. Consequently, searching for effective tumor markers is a central focus of LSCC research.

Due to the tissue and cell specificity of circular RNAs (circRNAs), they exert pivotal roles in various physiological and pathological processes [5, 6]. Abundant evidence

Correspondence: Yueyong Xiao, Chinese PLA General Hospital, No. 28 Fuxing Road, Haidian District, Beijing 100039, PR China, e-mail: szu9o5@sina.com; XianHua Zhu, Second Affiliated Hospital of Nanchang University, No. 1 Minde Road, Nanchang City 330000, Jiangxi Province, PR China, e-mail: zhuxianhuazxh@21cn.com
Submitted: 28.02.2025, Accepted: 30.06.2025

indicates that circRNAs have important functions in carcinogenesis, including cell proliferation and invasion [7, 8]. Currently, increasing circRNAs are associated with LSCC. For instance, circ_CORO1C is highly expressed in LSCC, and circ_CORO1C knockdown slows down LSCC progression by modulating miR-654-3p/USP7 [9]; hsa_circ_0036722 is lessened in LSCC and markedly associated with LSCC differentiation, implying that hsa_circ_0036722 acts as a potential diagnostic marker for LSCC [10]. Crucially, microarray analysis in previous research indicated that circRNAs (n = 302) are elevated in LSCC, and circRNAs (n = 396) are decreased [11]. Nevertheless, circRNA biological functions in LSCC have not been fully revealed. CircRNA High Mobility Group AT-hook 2 (circHMGA2, also named hsa_circ_0027446) is a newly identified circRNA and exhibits a cancer-promoting function. For example, circHMGA2 advances lung adenocarcinoma metastasis in both *in vitro* and *in vivo* models [12]; circHMGA2 is overexpressed in non-small cell lung cancer, and a high circHMGA2 level is associated with a poor prognosis in non-small cell lung cancer [13]. Until now, circHMGA2 function in LSCC remains unknown.

In this research, we identified a novel circRNA circHMGA2 in LSCC, which was elevated in LSCC, and high circHMGA2 expression was associated with TNM stage of LSCC patients. Thus, our studies further aimed to elucidate the biological function circHMGA2 in LSCC and its latent mechanism, in an attempt to provide a novel promising target for LSCC intervention.

Material and methods

Patient tissues

This prospective study included patients (n = 66) diagnosed with LSCC at our hospital between September 2022 and June 2023. All fresh tissues were stored at –80°C. The protocol was approved by the Institutional Ethical Review Committee of our hospital. Inclusion criteria: 1) All patients provided written informed consent; 2) All patients were diagnosed with LSCC for the first time; 3) None of the patients received chemotherapy or radiotherapy before the operation. Exclusion criteria: 1) LSCC patients with other diseases; 2) patients who have received chemotherapy or radiotherapy. Associations between circHMGA2 and LSCC patients' pathological characteristics (n = 66) are shown in Table 1.

Cell culture and co-culture assay

LSCC cells (TU686 and AMC-HN-8) were from ATCC (Manassas, USA). Human bronchial epithelioid cells (NP69) were supplied by Procell (Wuhan, China). All cells were placed in DMEM (Procell) with 10% FBS (Procell) and maintained at 37°C and 5% CO_2.

THP-1 cells were from ATCC and were placed in RPMI-1640 (Procell) with 10% FBS. THP-1 cells were exposed to 40 nM PMA (MedChemExpress, USA) to obtain M0 macrophages. Then, cells were exposed to 20 ng/ml interleukin (IL)-4 and 20 ng/ml IL-13 to obtain M2 macrophages [14]. Different groups of LSCC cell supernatant were co-cultured with M2 macrophages induced by

Table 1. Correlation between circHMGA2 expression and clinicopathological features of LSCC patients

Characteristic	All cases	circHMGA2 expression		*P*-value
		High (n = 33)	Low (n = 33)	
Age (years)				0.217
< 60	31	18	13	
≥ 60	35	15	20	
Gender				0.211
Male	27	16	11	
Female	39	17	22	
Tumor size (cm)				0.614
< 5	26	14	12	
≥ 5	40	19	21	
Lymphatic metastasis				0.013*
Yes	38	24	14	
No	28	9	19	
TNM stages				0.003**
I + II	38	13	25	
III + IV	28	20	8	

*$p < 0.05$, **$p < 0.01$

IL-4/IL-13 to investigate the effects of different groups of LSCC on M2 macrophage polarization [15].

Cell transfection

Sh-circHMGA2#1, sh-circHMGA2#2, sh-circHMGA2#3, and pcDNA3.1-ROCK1 were obtained from GenePharma (Shanghai, China). MiR-384 mimic and miR-384 inhibitor were from RiboBio (Guangzhou, China). LSCC cell transfection was conducted with Lipofectamine 2000 (Procell) [16].

Quantitative real-time polymerase chain reaction

Total RNA extraction was conducted with TRIzol (Thermo Fisher Scientific). The cDNA was synthesized using a Reverse Transcription Kit (Thermo Fisher Scientific) or miRNA cDNA Synthesis Kit (Thermo Fisher Scientific). Real-time PCR was conducted on a 7500 Real-Time PCR System (Applied Biosystems, USA) with SYBR Green I (Yeasen, Shanghai, China). Thermal cycles were: 95°C for 1 min, followed by 40 cycles at 95°C for 15 s, 60°C for 30 s, and 72°C for 30 s. U6 and GAPDH were the internal references. Gene levels were measured using $2^{-\Delta\Delta Ct}$. Primer sequences are presented in Table 2.

Table 2. Primer sequences

Gene name	Primer sequences (5′-3′)
CircHMGA2	Forward: GCCACTGGAGAAAAACGGCC
	Reverse: TTGCTGCCTTTGGGTCTTCC
CD206	Forward: TCTTTGCCTTTCCCAGTCTCC
	Reverse: TGACACCCAGCGGAATTTC
CD163	Forward: GGTGGACACAGAATGGTTCTTC
	Reverse: CCAGGAGCGTTAGTGACAGC
MiR-384	Forward: TGTTAAATCAGGAATTTTAA
	Reverse: TGTTACAGGCATTATGAA
ROCK1	Forward: GGTGGTCGGTTGGGGTATTTT
	Reverse: CGCCCTAACCTCACTTCCC
GAPDH	Forward: CAGGAGGCATTGCTGATGAT
	Reverse: GAAGGCTGGGGCTCATTT
U6	Forward: GCTTCGGCAGCACATATACT
	Reverse: GTGCAGGGTCCGAGGTATTC

Cell Counting Kit-8 assay

LSCC cells (1×10^3) were plated in 96-well plates and cultured for one day. Then Cell Counting Kit-8 (CCK-8) reagent (10 µl, Meilunbio, Dalian, China) was added and further cultured for 2 h. Eventually, absorbance at 450 nm was measured with a microplate reader (Thermo Fisher Scientific).

Cell invasion analysis

LSCC cell invasion was conducted using Transwell inserts coated with Matrigel (MBL, Beijing, China). LSCC cells (2×10^4) were added to the upper chamber of transwell inserts (8.0 µm, MBL). Medium with 20% FBS (Procell) was added to the lower chambers as a chemoattractant. Serum-free cell suspension was added to the upper chambers. Forty-eight hours later, non-invasive cells were removed and cells on the lower side were fixed using 4% paraformaldehyde (Thermo Fisher Scientific). Then cells were stained with 0.05% crystal violet (Shyuanye, Shanghai, China), and several invasive cells were counted with a microscope (Thermo Fisher Scientific).

Enzyme-linked immunosorbent assay

After LSCC cell supernatant was co-cultured with IL-4/IL-13-induced THP-1 cells, IL-10 and transforming growth factor β (TGF-β) levels in THP-1 cells were quantified using IL-10 enzyme-linked immunosorbent assay (ELISA) kits (Abcam) and TGF-β ELISA kits (YSRIBIO, Shanghai, China), following the reagent manufacturer's standard procedure.

Western blot

After proteins were extracted, protein contents were quantified using the BCA Protein Assay Kit (Beyotime, Shanghai, China). Proteins were dissociated with SDS-PAGE (GenScript, Nanjing, China) and were further transferred onto PVDF membranes (Shhk, Shanghai, China). After membranes were blocked, membranes were incubated with antibodies against IL-4 (1 : 1000, ab62351), CCL22 (MDC, 1 : 3000, ab124768), ARG1 (1 : 1000, ab315110), iNOS (1 : 1000, ab178945), TNF-α (1 : 1000, ab183218), TLR4 (1 : 1000, ab13556), ROCK1 (1 : 500, ab134181), and β-actin (ab8226) at 4°C. Later, membranes were exposed to secondary antibodies (1 : 2000, ab205718) for one hour. All antibodies were supplied by Abcam (Cambridge, UK). Protein bands were visualized using enhanced chemiluminescence (ECL; Thermo Fisher Scientific).

Database analysis

Putative binding sites of circHMGA2 and miR-384 were predicted using Circinteractome (https://circinteractome.nia.nih.gov/index.html). Also, the presence of miR-384 binding sites in the 3′ untranslated region of ROCK1 was predicted by StarBase (http://starbase.sysu.edu.cn/).

Dual-luciferase reporter assay

CircHMGA2-wild type (WT), circHMGA2-mutant (MUT), ROCK1-WT, and ROCK1-MUT were synthesized by RiboBio (Guangzhou, China). CircHMGA2-WT, circHMGA2-MUT, ROCK1-WT, and ROCK1-MUT were cloned into pGL3-promoter (Promega, USA). Luciferase reporter plasmids and miR-384 mimic were transfected into LSCC cells with Lipofectamine 2000 as per the supplier's instructions. Relative luciferase activity was tested by the Dual-Luciferase Reporter Assay System (Promega).

RNA pull-down

A biotin-labeled circHMGA2 probe (Sangon, Shanghai, China) and a bio-NC probe (Sangon) were applied for RNA pull-down assay. After the LSCC cell lysate was obtained, it was further incubated with a bio-circHMGA2 probe at 4°C. One night later, the RNA complex that was bound to beads was eluted, the mixture was exposed to TRIzol for RNA extraction, and miR-384 expression was tested.

Tumor xenograft experiments

BALB/C nude mice (6-8 weeks) were supplied by Gempharmatech (Nanjing, China). This research was approved by the Ethics Committee of the Second Affiliated Hospital of Nanchang University and was conducted given ARRIVE guidelines (https://arriveguidelines.org).

For the instruction of xenograft tumor models, AMC-HN-8 cells transfected with sh-circHMGA2 (1×10^7 cells) were subcutaneously inoculated into nude mice [17]. Six mice were assigned to each group. Subcutaneous tumor size was tested every 7 days between 7 and 28 days. Tumor volume was quantified according to the following formula: V (volume) = (length × width^2)/2. After five weeks, all mice were sacrificed.

Hematoxylin-eosin staining and immunohistochemistry assays

LSCC tissues were fixed in 4% paraformaldehyde, embedded in paraffin, and cut into 5-μm sections. Subsequently, sections were exposed to hematoxylin and eosin (Solarbio, Beijing, China).

LSCC tissues were fixed with 4% paraformaldehyde, embedded in paraffin, and cut into 5-μm sections. Then the sections were exposed to antibodies against Ki-67 (1 : 200, ab16667), CD206 (Mannose Receptor, Abcam, 0.1 μg/ml), and CD163 (Abcam, 1 : 500) at 4°C. Next, sections were washed and exposed to secondary antibodies (Abcam) at room temperature. Then sections were stained using DAB (Solarbio) and further counterstained with hematoxylin (Solarbio).

Statistical analysis

All data were presented as mean ± SD. Student's *t*-test or one-way ANOVA test followed by Tukey's post hoc test was applied to compare two or multiple groups. Survival curves were determined using Kaplan-Meier analysis. The relationship between circHMGA2 expression and LSCC clinicopathological characteristics was assessed by the chi-square test. $P < 0.05$ was considered to indicate statistical significance.

Results

High expression of circHMGA2 in LSCC

To investigate the role of circHMGA2 in mediating LSCC, we evaluated circHMGA2 expression in LSCC and found that circHMGA2 was overexpressed in LSCC tissues (Fig. 1A). Kaplan-Meier survival curve analysis further confirmed that overall survival of patients with elevated circHMGA2 levels was shorter (Fig. 1B). Meanwhile, elevated circHMGA2 expression was associated with TNM stage, but not with LSCC patients' age, gender, tumor size, or lymphatic metastasis (Table 1). Also, circHMGA2 levels in LSCC cells (TU686 and AMC-HN-8 cells) were more than four times higher than those in NP69 cells (Fig. 1C). Overall, circHMGA2 was raised in LSCC.

CircHMGA2 knockdown suppresses LSCC proliferation and invasion and inhibits M2 macrophage polarization

The biological function of circHMGA2 in LSCC cells was further examined. First, circHMGA2 was knocked down in LSCC cells, and transfection efficiency verification revealed that sh-circHMGA2#1, #2, and #3 effectively reduced circHMGA2 levels in LSCC cells (Fig. 2A). sh-circHMGA2#1 (named sh-circHMGA2) showed the highest knockdown efficiency and was applied in our research. CCK-8 further demonstrated that silencing circHMGA2 reduced LSCC cell proliferation (Fig. 2B).

Additionally, circHMGA2 knockdown attenuated LSCC cell invasion ability (Fig. 2C, D). After LSCC cell supernatant was co-cultured with IL-4/IL-13-induced THP-1 cells, we further confirmed that circHMGA2 knockdown reduced levels of M2 macrophage marker molecules CD206 and CD163 in cells (Fig. 2E), and reduced M2 representative cytokines IL-10 and TGF-β contents (Fig. 2F). Meanwhile, circHMGA2 knockdown reduced the protein levels of M2 macrophage markers IL-4, CCL22, and ARG1 (Fig. 2G) and increased the protein levels of M1 macrophage markers iNOS, TNF-α, and TLR4 (Fig. 2H). These findings implied that circHMGA2 knockdown inhibited LSCC cell proliferation and invasion, and repressed M2 macrophage polarization.

CircHMGA2 targets miR-384

As shown in Figure 3A, circHMGA2 contains miR-384 binding sites. MiR-384 expression was confirmed to markedly rise after transfecting miR-384 mimic into

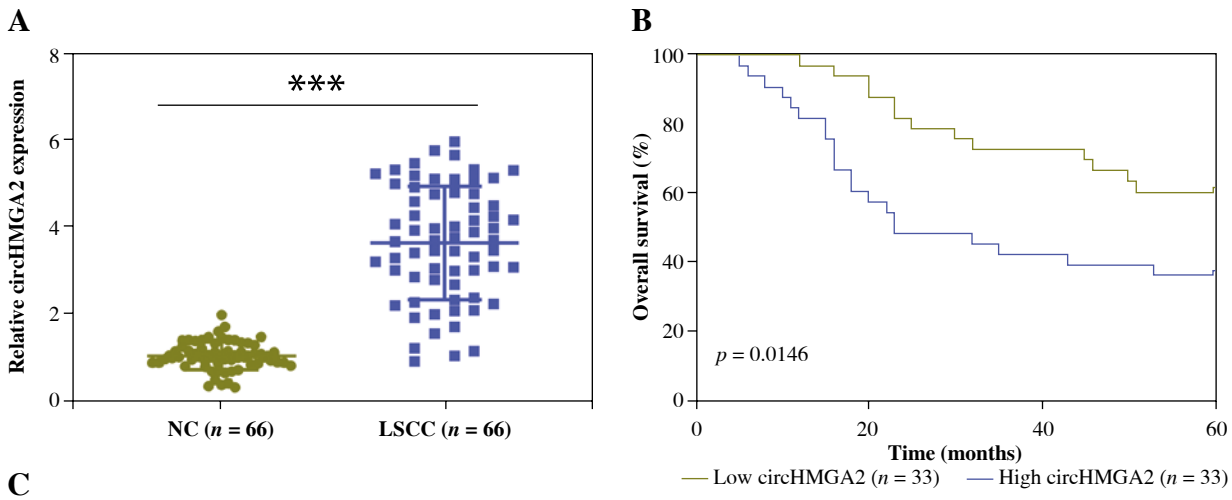

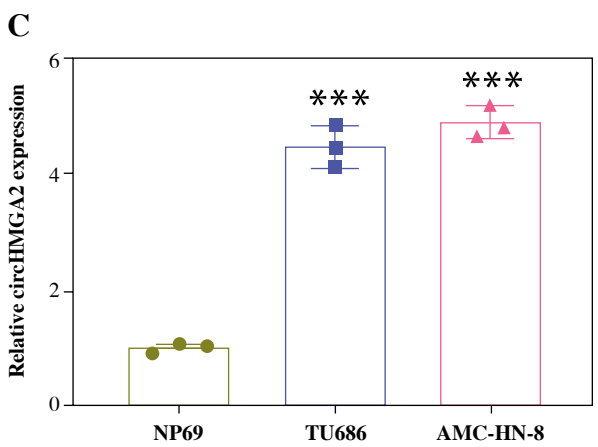

Fig. 1. Validation of circHMGA2 expression in LSCC tissues and cells. **A**) Analysis of circHMGA2 expression in LSCC tissues and adjacent tissues ($n = 66$) using quantitative real-time polymerase chain reaction (qRT-PCR). **B**) Median value of circHMGA2 expression in LSCC ($n = 66$) was set as a cut-off value. The association between circHMGA2 and the overall survival rate of LSCC was examined *via* Kaplan-Meier analysis. **C**) Detection of circHMGA2 expression in LSCC cells (TU686 and AMC-HN-8 cells) and human bronchial epithelioid cells (NP69) using qRT-PCR. ***$p < 0.001$ vs. NC, NP69 cells. NC – negative control

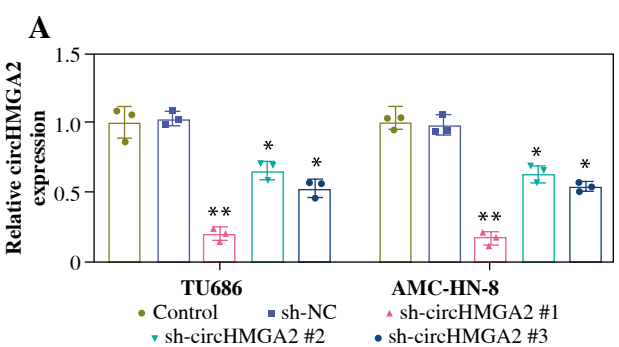

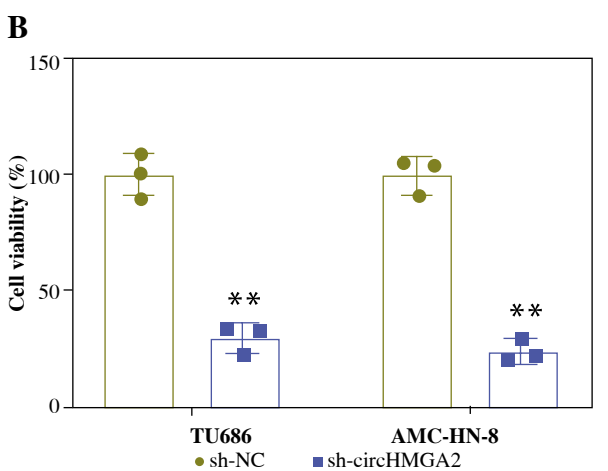

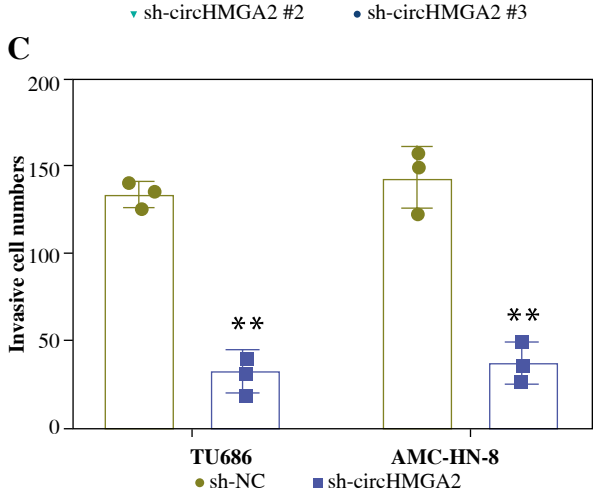

Fig. 2. CircHMGA2 mediates LSCC cell proliferation and invasion and regulates M2 macrophage polarization. **A**) Sh-circHMGA2#1, #2, or #3 was transfected into LSCC cells for 48 h. Detection of circHMGA2 expression using qRT-PCR. **B**) Sh-circHMGA2#1 (sh-circHMGA2) was transfected into LSCC cells for 48 h. LSCC cell proliferation was determined by Cell Counting Kit-8 (CCK-8). **C**) LSCC cell invasion was estimated *via* Transwell (scale bar: 100 μM). *$p < 0.05$, **$p < 0.01$ vs. sh-NC

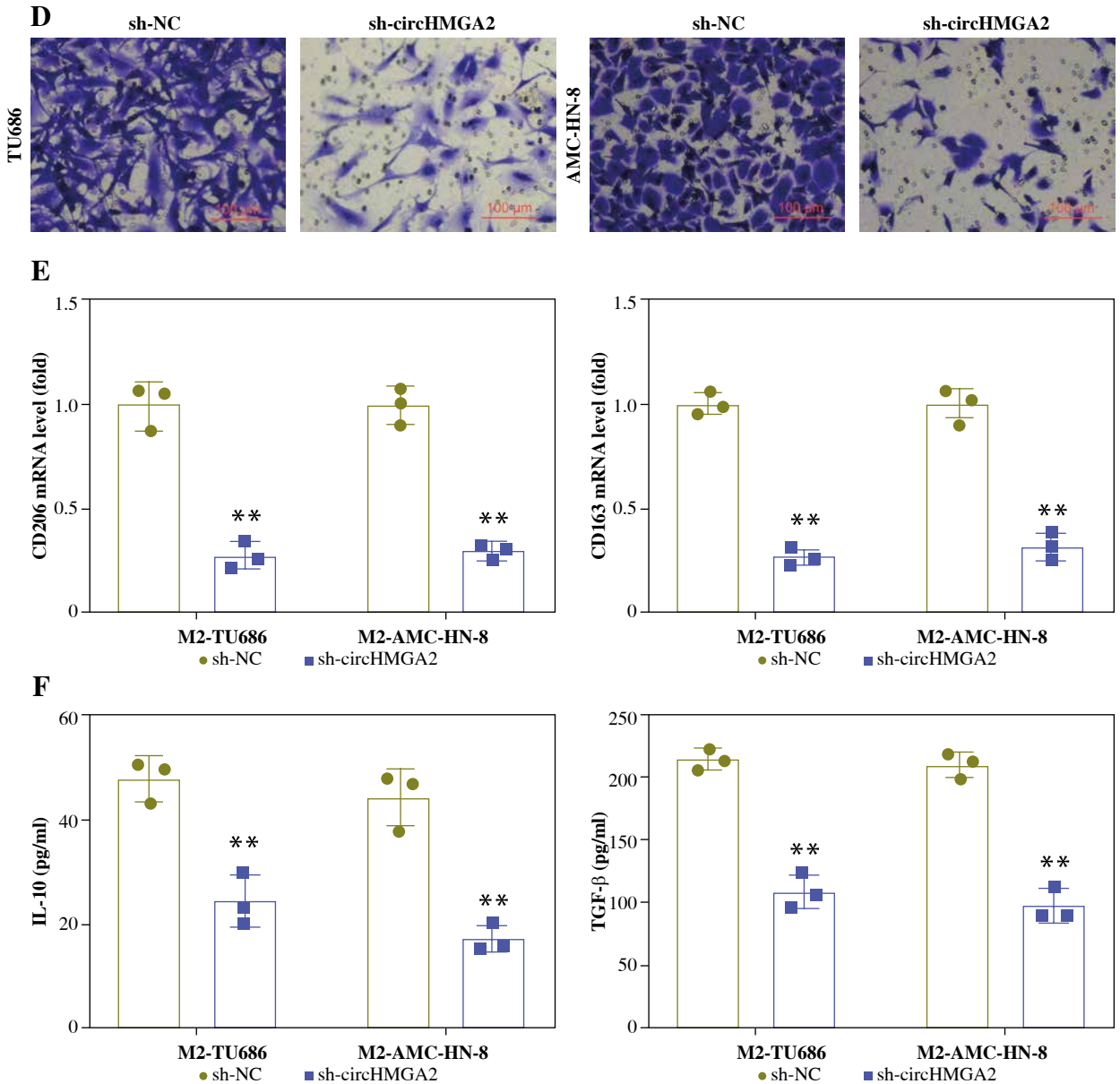

Fig. 2. Cont. **D**) LSCC cell invasion was estimated *via* Transwell (scale bar: 100 μM). **E**) THP-1 cells were treated with 40 nM PMA to obtain M0 macrophages; the cells were then exposed to 20 ng/ml IL-4 and 20 ng/ml IL-13 to obtain M2 macrophages. LSCC cell supernatant was further co-cultured with M2 macrophages induced by IL-4/IL-13. CD206 and CD163 expression levels were determined with qRT-PCR. **F**) Comparison of M2 representative cytokines IL-10 and TGF-β concentrations by enzyme-linked immunosorbent assay (ELISA). *$p < 0.05$, **$p < 0.01$ vs. sh-NC

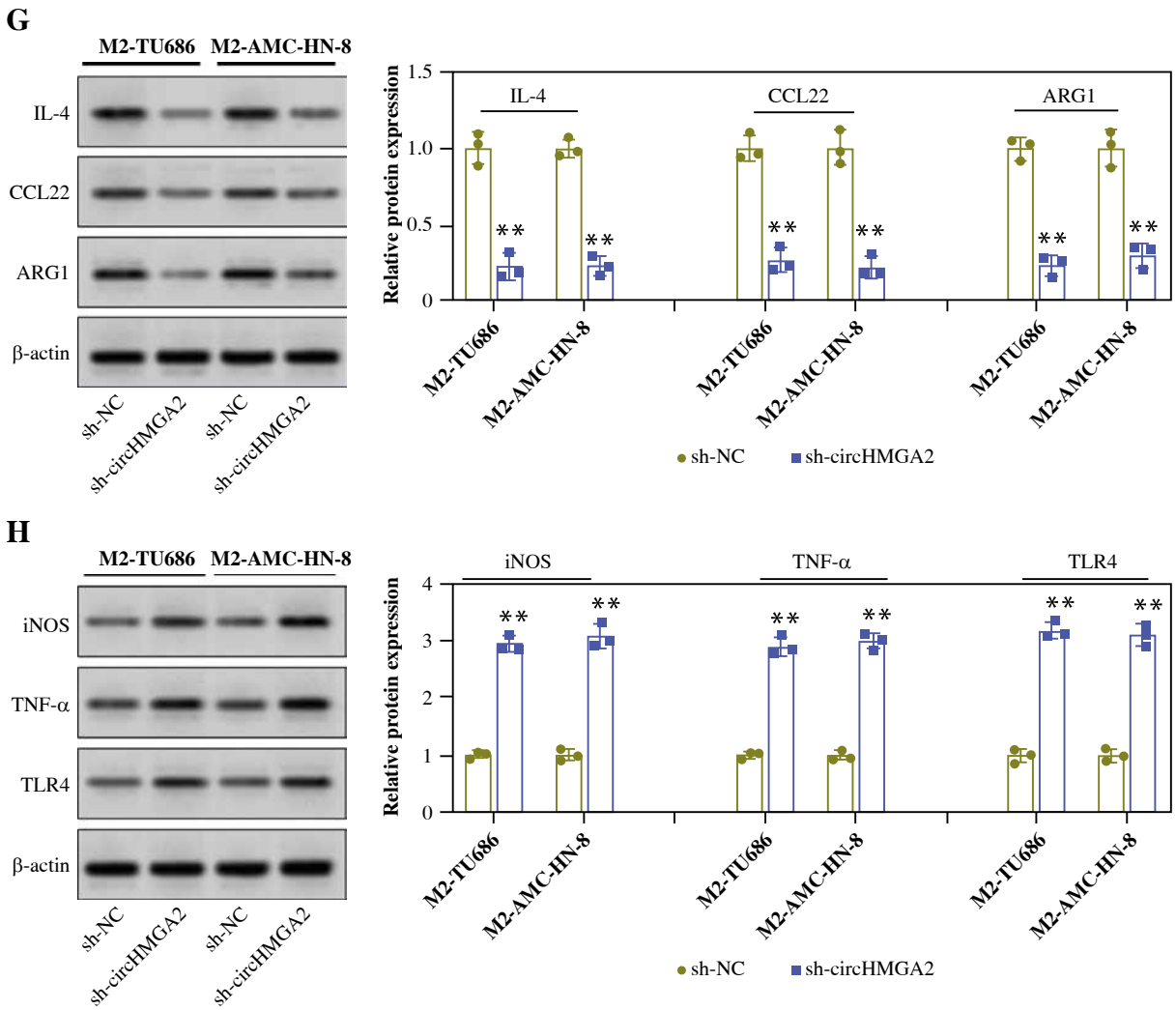

Fig. 2. Cont. **G**, **H**) Analysis of protein levels of M2 macrophage markers (IL-4, CCL22, and ARG1) and M1 macrophage markers (iNOS, TNF-α, and TLR4) using Western blot. *$p < 0.05$, **$p < 0.01$ vs. sh-NC

TU686 and AMC-HN-8 cells (Fig. 3B). On this basis, we further found that luciferase activity was lessened in circHMGA2-WT by nearly 75% in response to miR-384 overexpression, and luciferase activity showed no significant changes in circHMGA2-MUT (Fig. 3C). Also, the bio-circHMGA2 probe enriched more miR-384 in comparison with the NC probe (Fig. 3D). Meanwhile, miR-384 expression was decreased in LSCC tissues (Fig. 3E), and miR-384 was negatively correlated with circHMGA2 expression in LSCC tissues (Fig. 3F). Hence, miR-384 was the downstream target of circHMGA2.

MiR-384 modulates ROCK1 expression

Subsequently, downstream regulatory molecules of miR-384 were further investigated. As shown in Figure 4A, miR-384 binding sites are located in the 3′ untranslated region of ROCK1. Also, miR-384 mimic reduced luciferase activity in LSCC cells, and this reduction disappeared after mutation of the predicted binding sites (Fig. 4B). Additionally, miR-384 overexpression reduced ROCK1 protein level in LSCC cells (Fig. 4C). Then, miR-384 inhibitor was verified to transfect into LSCC cells (Fig. 4D). Based on these findings, we further corroborated that sh-circHMGA2 decreased ROCK1 protein level, and co-transfection with miR-384 inhibitor abolished this decrease (Fig. 4E). Also, ROCK1 expression was higher in LSCC than that in adjacent tissues (Fig. 4F). We additionally observed that miR-384 was negatively associated with ROCK1 expression in LSCC ($r = –0.6431$, $p < 0.001$, Fig. 4G), while circHMGA2 was positively associated with ROCK1 expression ($r = 0.5436$, $p < 0.001$, Fig. 4H). Collectively, these results show that miR-384 negatively regulated ROCK1 expression in LSCC.

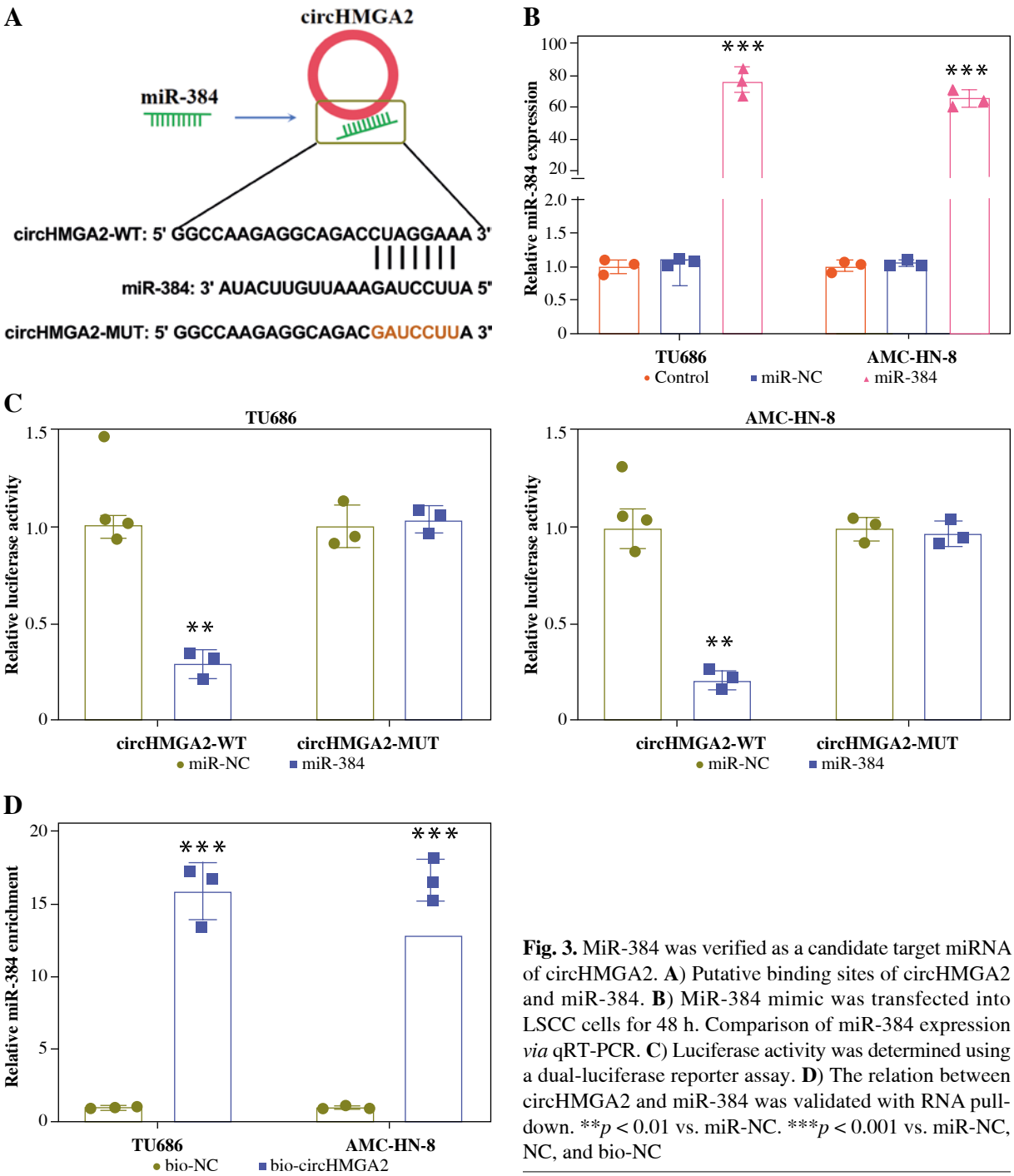

Fig. 3. MiR-384 was verified as a candidate target miRNA of circHMGA2. **A**) Putative binding sites of circHMGA2 and miR-384. **B**) MiR-384 mimic was transfected into LSCC cells for 48 h. Comparison of miR-384 expression *via* qRT-PCR. **C**) Luciferase activity was determined using a dual-luciferase reporter assay. **D**) The relation between circHMGA2 and miR-384 was validated with RNA pull-down. $^{**}p < 0.01$ vs. miR-NC. $^{***}p < 0.001$ vs. miR-NC, NC, and bio-NC

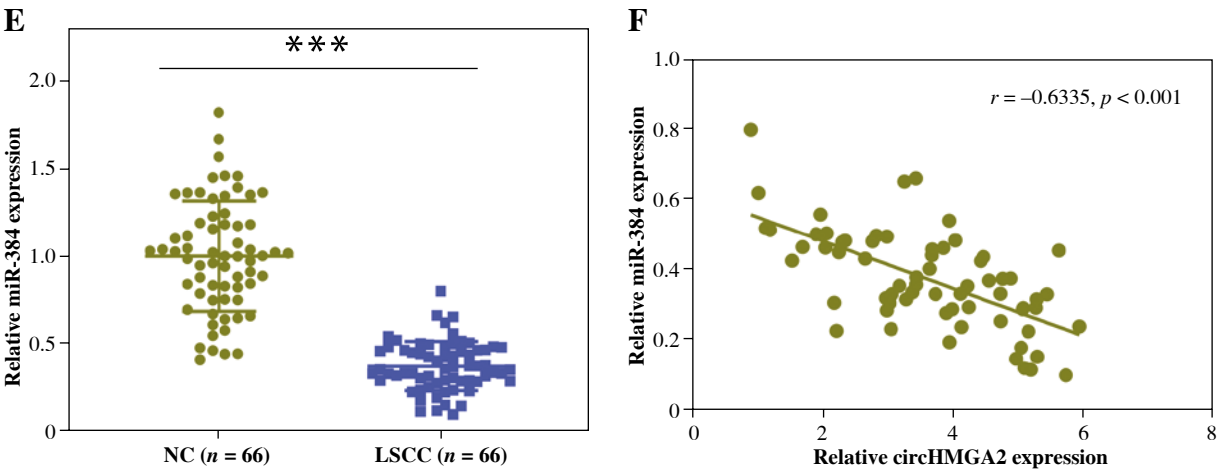

Fig. 3. Cont. **E**) Analysis of miR-384 expression in LSCC tissues and adjacent tissues (n = 66) using qRT-PCR. **F**) Correlation between miR-384 and circHMGA2 expression in LSCC tissues. $^{**}p < 0.01$ vs. miR-NC. $^{***}p < 0.001$ vs. miR-NC, NC, and bio-NC

CircHMGA2 mediates LSCC progression through miR-384/ROCK1

We further examined whether circHMGA2 modulated the LSCC process *via* miR-384/ROCK1. After ROCK1 was successfully overexpressed in LSCC (Fig. 5A), CCK-8 further demonstrated that circHMGA2 knockdown attenuated LSCC cell proliferation ability by nearly 75%, while co-transfection of miR-384 inhibitor or pcDNA3.1-ROCK1 abolished this trend (Fig. 5B). LSCC cell invasion analysis displayed a similar trend (Fig. 5C, D). Additionally, circHMGA2 knockdown reduced CD206 and CD163 levels in THP 1 cells, and this decrease was abolished after transfecting miR-384 inhibitor or pcDNA3.1-ROCK1 (Fig. 5E).

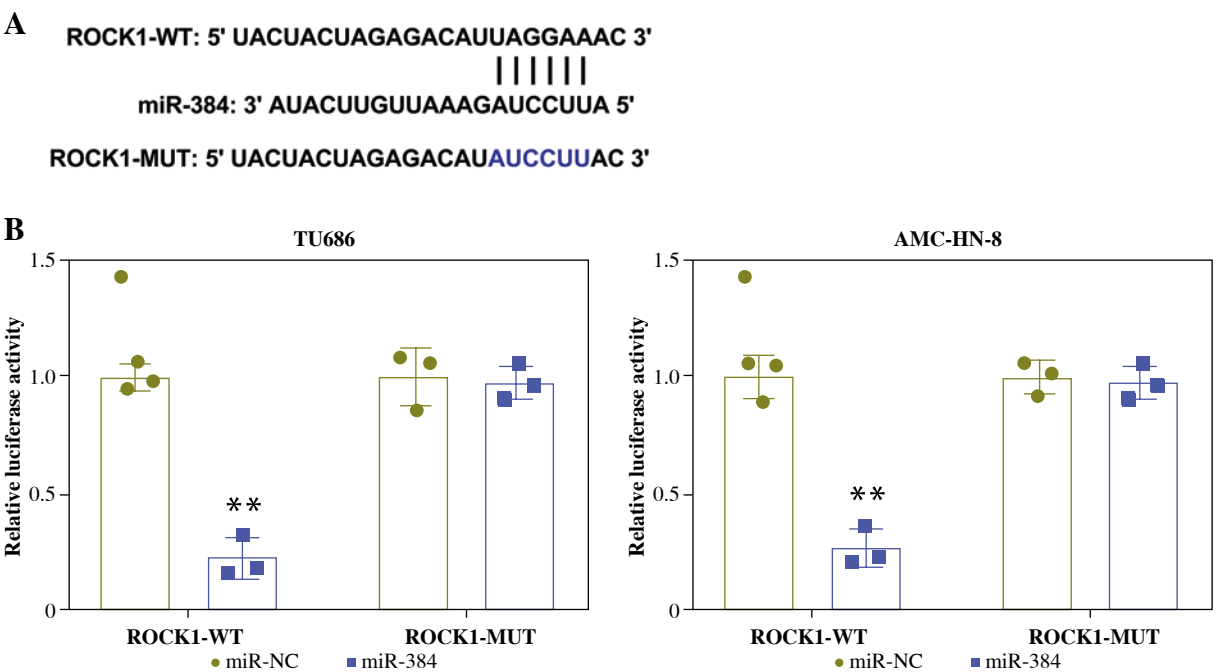

Fig. 4. MiR-384 mediates ROCK1 expression. **A**) StarBase predicted the presence of miR-384 binding sites in the 3′ untranslated region of ROCK1. **B**) Analysis of luciferase activity in LSCC cells by dual-luciferase reporter assay. $^{**}p < 0.01$ vs. miR-NC, NC inhibitor, and sh-NC; $^{***}p < 0.001$ vs. NC; $^{\#\#}p < 0.01$ vs. sh-circHMGA2

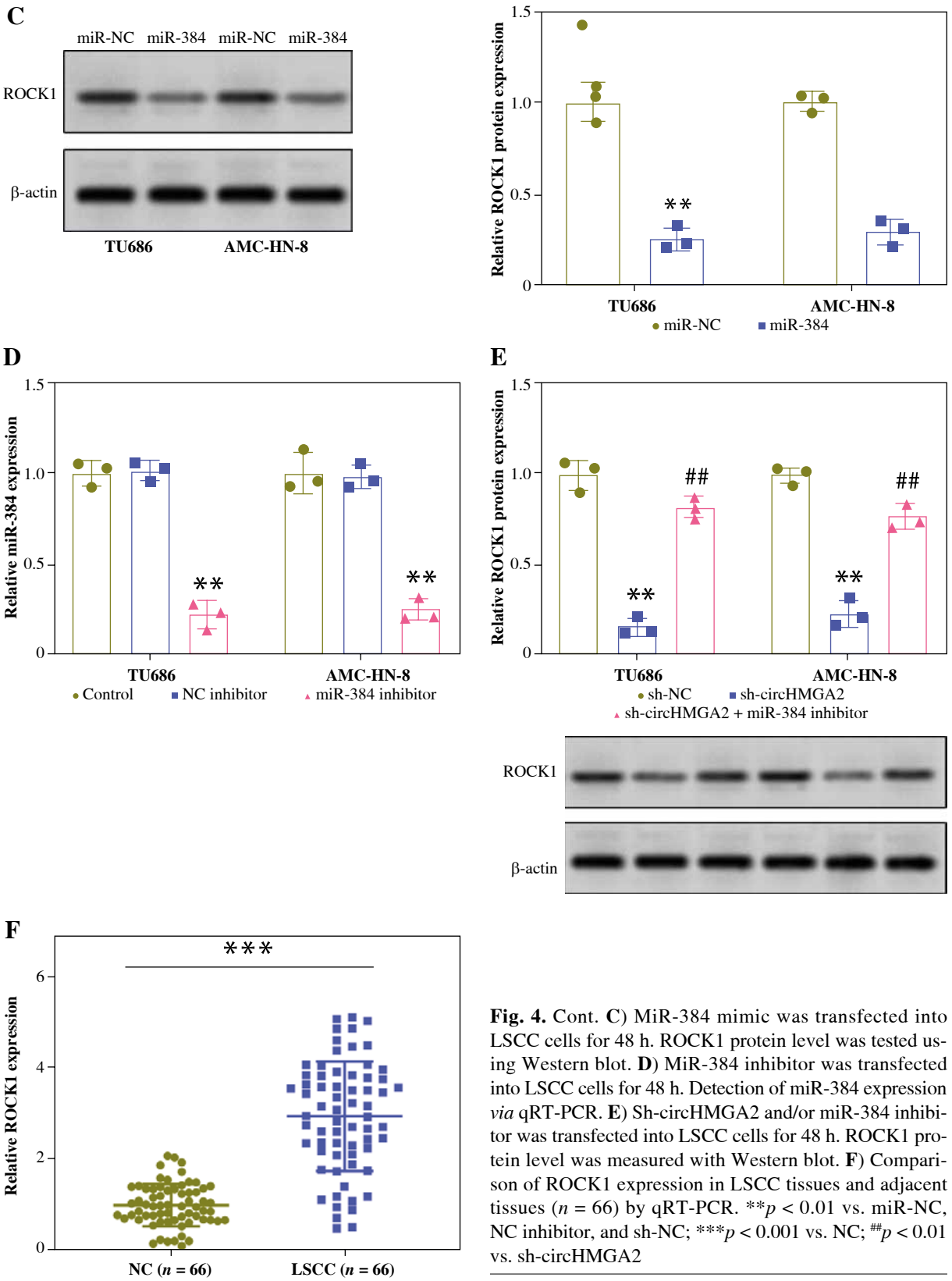

Fig. 4. Cont. **C**) MiR-384 mimic was transfected into LSCC cells for 48 h. ROCK1 protein level was tested using Western blot. **D**) MiR-384 inhibitor was transfected into LSCC cells for 48 h. Detection of miR-384 expression *via* qRT-PCR. **E**) Sh-circHMGA2 and/or miR-384 inhibitor was transfected into LSCC cells for 48 h. ROCK1 protein level was measured with Western blot. **F**) Comparison of ROCK1 expression in LSCC tissues and adjacent tissues (n = 66) by qRT-PCR. $^{**}p < 0.01$ vs. miR-NC, NC inhibitor, and sh-NC; $^{***}p < 0.001$ vs. NC; $^{\#\#}p < 0.01$ vs. sh-circHMGA2

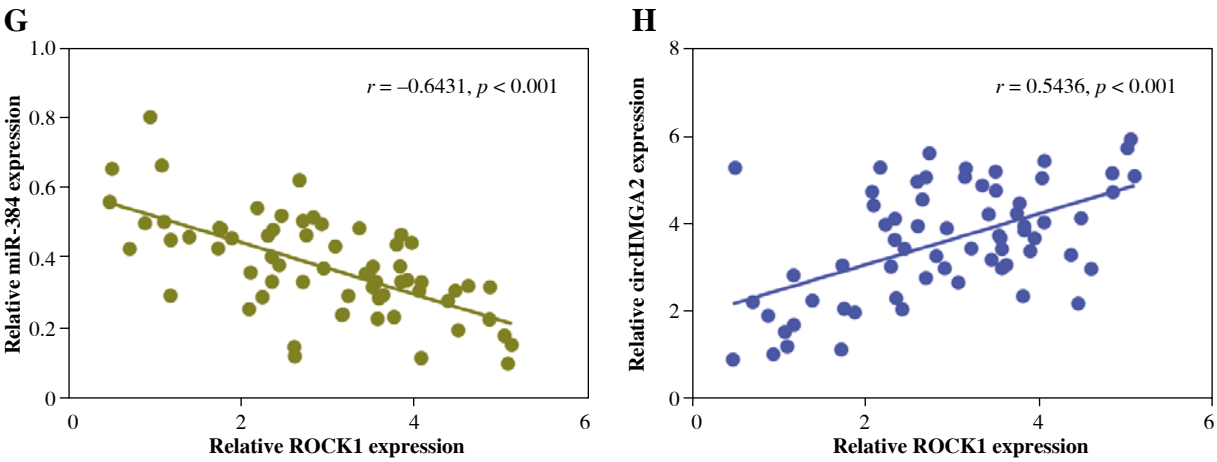

Fig. 4. Cont. **G**, **H**) Correlation between miR-384 and ROCK1 expression, circHMGA2 and ROCK1 expression in LSCC tissues. $^{**}p < 0.01$ vs. miR-NC, NC inhibitor, and sh-NC; $^{***}p < 0.001$ vs. NC; $^{\#\#}p < 0.01$ vs. sh-circHMGA2

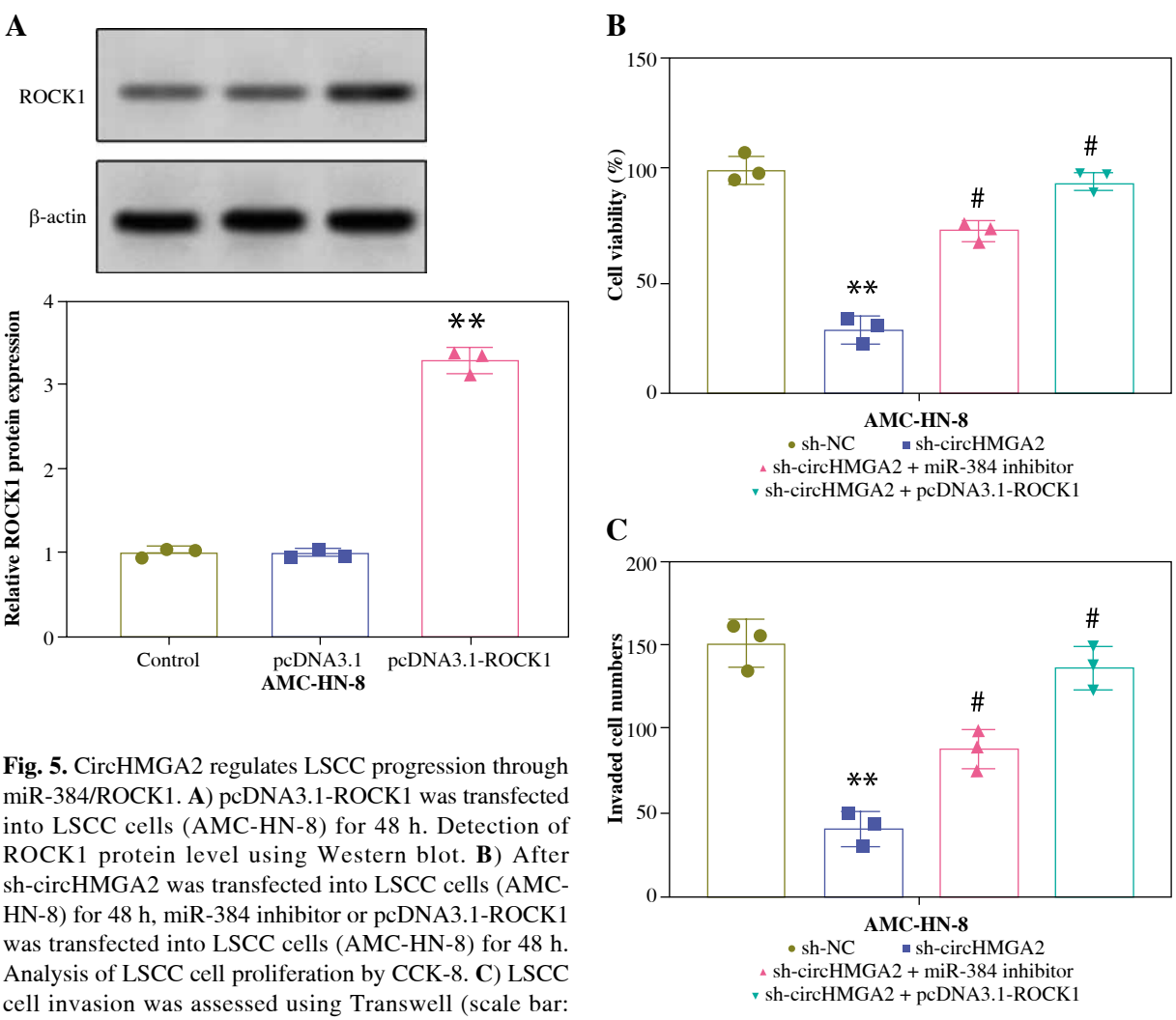

Fig. 5. CircHMGA2 regulates LSCC progression through miR-384/ROCK1. **A**) pcDNA3.1-ROCK1 was transfected into LSCC cells (AMC-HN-8) for 48 h. Detection of ROCK1 protein level using Western blot. **B**) After sh-circHMGA2 was transfected into LSCC cells (AMC-HN-8) for 48 h, miR-384 inhibitor or pcDNA3.1-ROCK1 was transfected into LSCC cells (AMC-HN-8) for 48 h. Analysis of LSCC cell proliferation by CCK-8. **C**) LSCC cell invasion was assessed using Transwell (scale bar: 100 μM). $^{**}p < 0.01$ vs. vector, sh-NC; $^{\#}p < 0.05$ vs. sh-circHMGA2

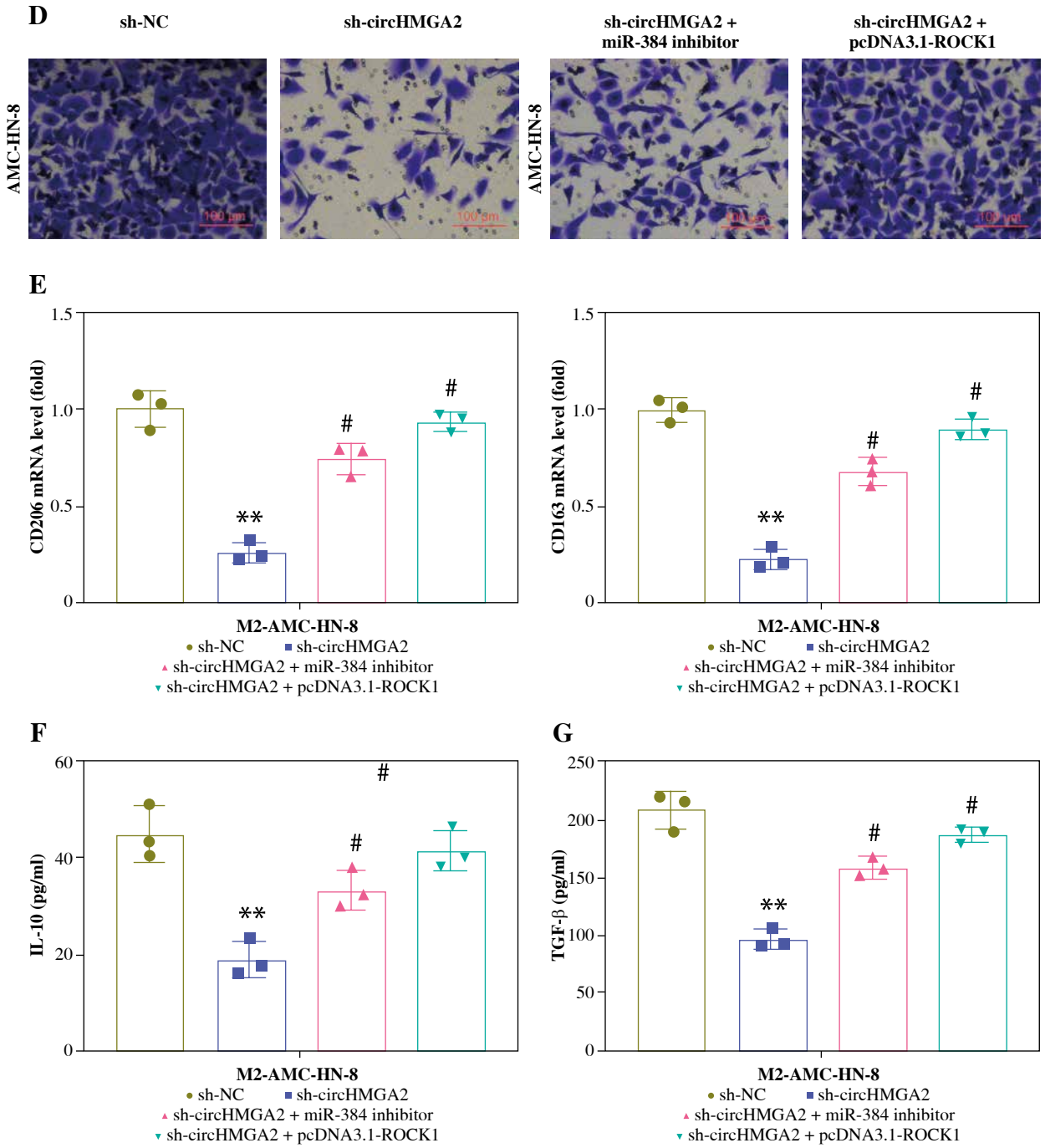

Fig. 5. Cont. **D**) LSCC cell invasion was assessed using Transwell (scale bar: 100 μM). **E**) After exposing THP-1 cells to 40 nM PMA to obtain M0 macrophages, the cells were treated with 20 ng/ml IL-4 and 20 ng/ml IL-13 to obtain M2 macrophages. LSCC cell supernatant was then co-cultured with M2 macrophages induced by IL-4/IL-13. Comparison of CD206 and CD163 expression by qRT-PCR. **F**, **G**) IL-10 and TGF-β concentrations were tested using ELISA. $^{**}p < 0.01$ vs. vector, sh-NC; $^{\#}p < 0.05$ vs. sh-circHMGA2

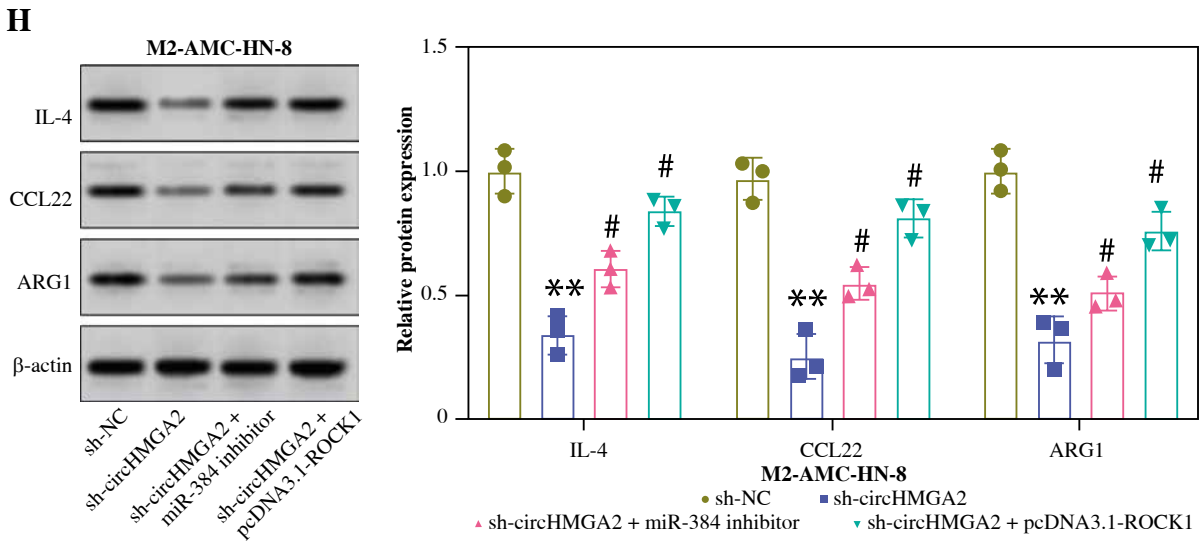

Fig. 5. Cont. **H**) Protein levels of M2 macrophage markers (IL-4, CCL22, and ARG1) were tested using Western blot. $^{**}p < 0.01$ vs. vector, sh-NC; $^{\#}p < 0.05$ vs. sh-circHMGA2

Moreover, circHMGA2 knockdown reduced IL-10 and TGF-β expression, while transfecting miR-384 inhibitor or pcDNA3.1-ROCK1 abolished these trends (Fig. 5F, G). Silencing of circHMGA2 decreased the protein levels of M2 macrophage markers IL-4, CCL22, and ARG1, but miR-384 inhibitor or pcDNA3.1-ROCK1 abolished this decrease (Fig. 5H). The above findings suggest that circHMGA2 promotes the malignant phenotype of LSCC *via* the miR-384/ROCK1 axis.

Interference with circHMGA2 reduces LSCC proliferation and suppresses M2 polarization *in vivo*

To further inquire whether circHMGA2 modulated LSCC growth *in vivo*, AMC-HN-8 cells transfected with sh-circHMGA2 were subcutaneously inoculated into nude mice. As shown in Figure 6A, sh-circHMGA2 resulted in reduced subcutaneous tumorigenesis in nude mice. Also, circHMGA2 knockdown did not markedly change the weight of mice (Fig. 6B), but markedly reduced tumor weight (Fig. 6C). HE staining further revealed that circHMGA2 knockdown reduced the number of lesions (Fig. 6D). Also, the positive staining rates of Ki-67, CD206, and CD163 in LSCC tissues were decreased after knocking down circHMGA2 (Fig. 6D, E). Meanwhile, circHMGA2 knockdown reduced circHMGA2 expression, and elevated miR-384 expression in LSCC tissues (Fig. 6F), while lowering ROCK1 protein levels in LSCC tissues (Fig. 6G). To sum up, our experimental data indicate that circHMGA2 promotes the malignant biological phenotype and M2 macrophage polarization *via* the miR-384/ROCK1 axis in LSCC (Fig. 7). In general, sh-circHMGA2 inhibited LSCC growth and reduced M2 polarization *in vivo*.

Discussion

Laryngeal squamous cell carcinoma is a highly aggressive malignancy [18], and there is an urgent need to understand the mechanisms involved in LSCC. In the past few decades, the specific biological functions of circRNAs in cancer have attracted various concerns [19, 20]. Nevertheless, circRNA functions in LSCC have not been fully revealed. Here, we discovered that a novel circRNA, circHMGA2, was higher in LSCC tissues than in adjacent tissues, and elevated circHMGA2 expression was associated with the TNM stage of LSCC patients, and patients with high circHMGA2 had shorter overall survival. Similar to this finding, circHMGA2 can be applied as a therapeutic target for lung adenocarcinoma [12]. Also, functional data suggested that circHMGA2 knockdown repressed LSCC proliferation and invasion, and circHMGA2 knockdown reduced M2 macrophage polarization. Mechanistic data further demonstrated that circHMGA2 modulated LSCC malignant phenotype *via* miR-384/ROCK1. All these findings strongly suggest that circHMGA2 is a novel circRNA that exerts oncogenic activity in LSCC.

Considering the significance of circRNAs in LSCC research [21, 22], this study sought to identify more circRNAs that function in LSCC. In the current research, circHMGA2 was raised in LSCC. Also, circHMGA2 knockdown weakened LSCC proliferation and invasion. Previous studies have demonstrated that M2 macrophages are macrophage phenotypes, and accelerate tumor cell

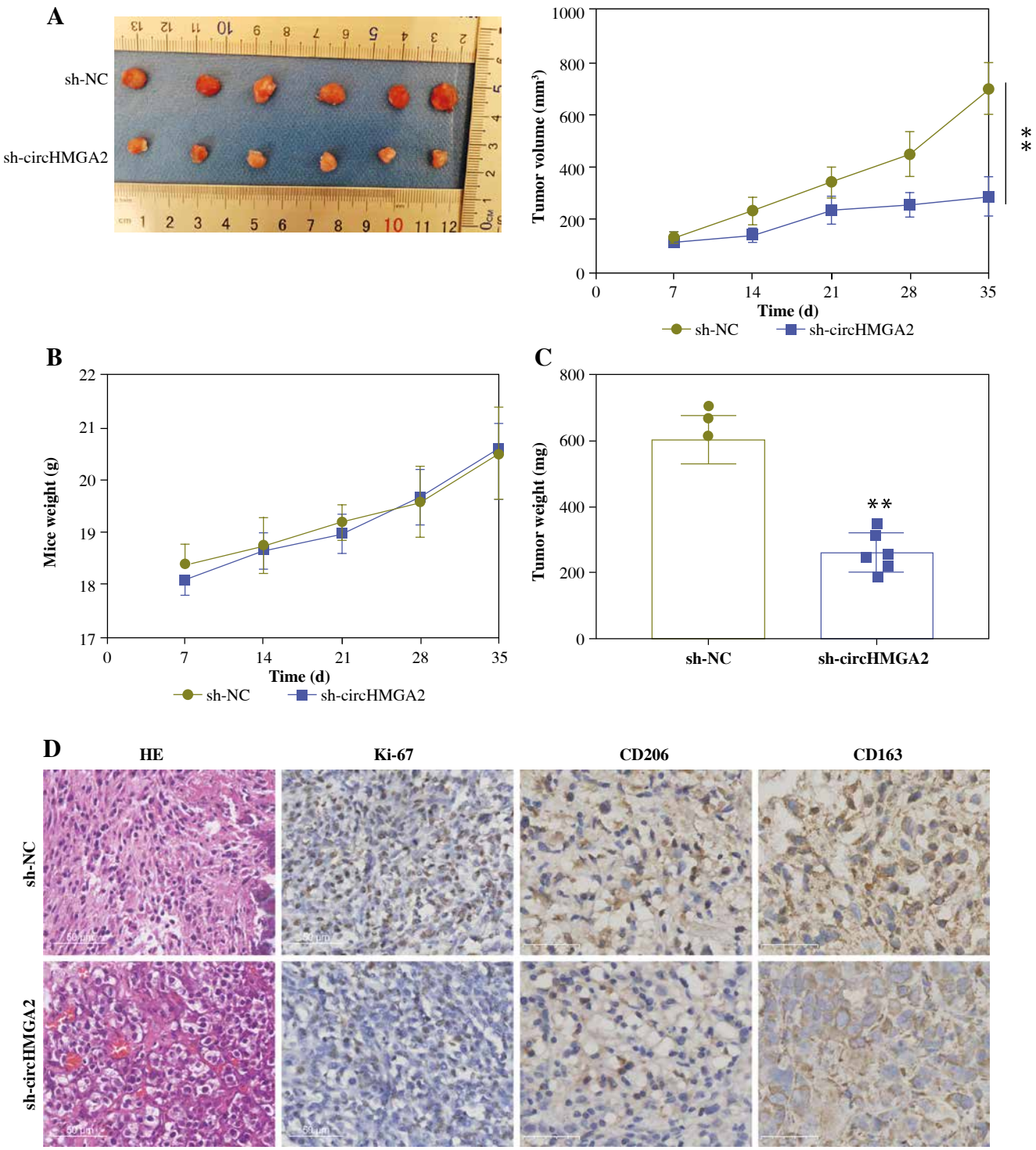

Fig. 6. CircHMGA2 mediates LSCC proliferation and M2 polarization *in vivo*. AMC-HN-8 cells transfected with sh-circHMGA2 (1×10^7 cells) were subcutaneously inoculated into nude mice. **A**) Analysis of mouse tumor volume. **B**) Measurement of weight of mice. **C**) Comparison of mouse tumor weight. $^{**}p < 0.01$ vs. sh-NC. **D**) Number of lesions was determined using hematoxylin-eosin (HE) staining (scale bar: 50 μM).

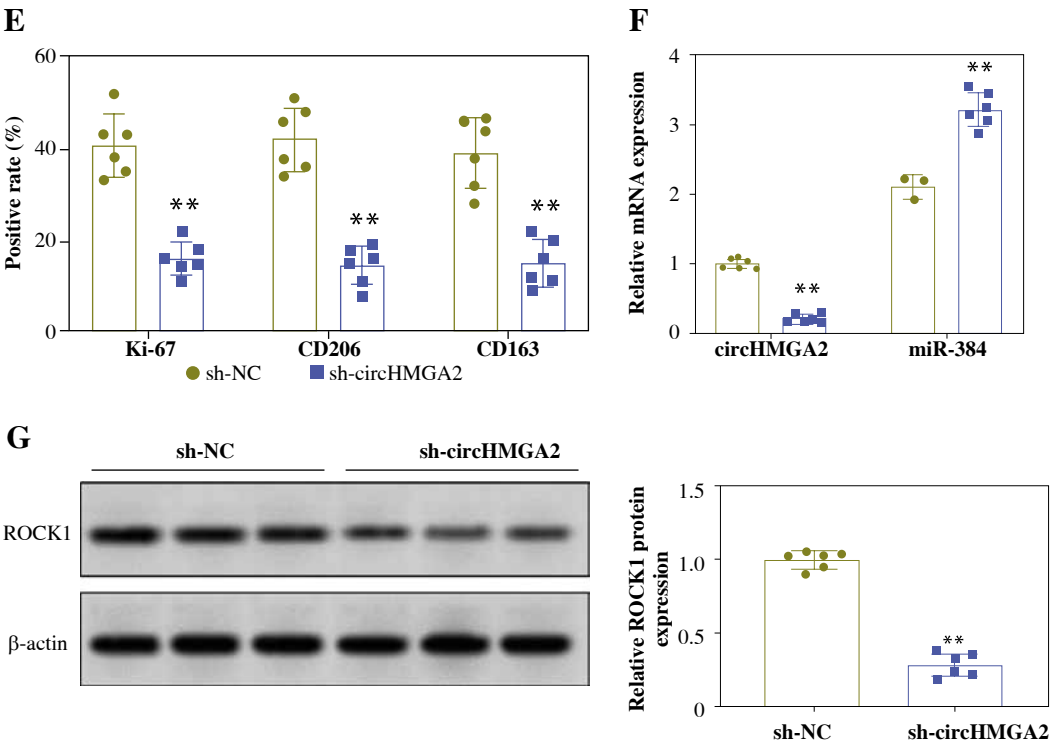

Fig. 6. Cont. **E**) Ki-67, CD206, and CD163 expression levels were measured by immunohistochemistry (scale bar: 50 μM). **F**) Comparison of circHMGA2 and miR-384 expression by qRT-PCR. **G**) ROCK1 protein level was tested using Western blot. $^{**}p < 0.01$ vs. sh-NC

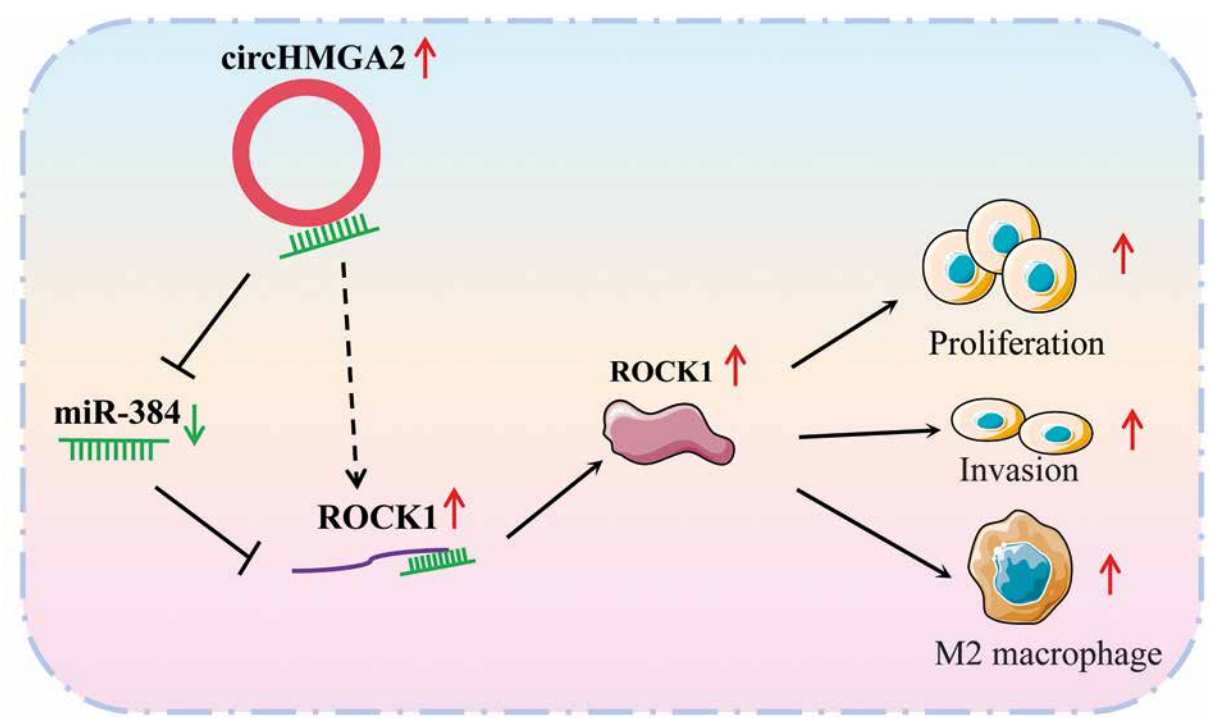

Fig. 7. CircHMGA2 promotes the malignant biological phenotype and M2 macrophage polarization *via* miR-384/ROCK1 axis in LSCC

growth and carcinogenesis in a tumor microenvironment [23, 24]. As has been reported, M2 macrophages express CD163 and CD206 [25]. Our study showed that circHMGA2 knockdown reduced CD163 and CD206 expression in LSCC cells. IL-4, CCL22, and ARG1 are M2 macrophage markers, and iNOS, TNF-α, and TLR4 are M1 macrophage markers [26, 27]. This research further indicated that silencing circHMGA2 reduced protein levels of the M2 macrophage markers IL-4, CCL22, and ARG1, while increasing protein levels of the M1 macrophage markers iNOS, TNF-α, and TLR4, suggesting that circHMGA2 knockdown inhibited M2 macrophage polarization.

Subsequently, we elucidated the mechanism by which circHMGA2 functions in LSCC. Numerous studies indicate that circRNAs block the inhibitory function of target genes by absorbing microRNAs (miRNAs) [28, 29]. Abnormal expression of miRNAs is associated with LSCC progression. For instance, array analysis demonstrated that miR-31 and let-7a are overexpressed in LSCC, and they are applied to diagnose LSCC patients with high sensitivity and specificity [30]; miR-196b is raised in LSCC, and miR-196b expression is associated with histological grade and TNM stage of LSCC patients [31]. Critically, circRNAs act as sponges for miRNAs, sequestering them and thereby restraining their functions. For instance, Wei *et al*. demonstrated that hsa_circ_0042666 modulates LSCC cell growth via competitively binding to miR-223, and provides a novel LSCC therapeutic strategy [32]; also, Yin *et al*. reported that circZNF609 knockdown weakens LSCC cell proliferation and invasion *via* absorbing miR-134-5 [33]. Meanwhile, miR-384 is modulated by multiple circRNAs in different human diseases [34, 35]. Here, we preliminarily confirmed that miR-384 was the downstream target of circHMGA2, and miR-384 showed low expression in LSCC. Furthermore, our experimental data indicated that miR-384 was negatively associated with circHMGA2 expression in LSCC tissues. These data suggest that circHMGA2 has oncogenic function in LSCC through sponging miR-384.

To further define a latent mechanism for miR-384, miR-384 targets were predicted. We preliminarily determined that ROCK1 was an LSCC target through StarBase and dual-luciferase reporter assay. Previously, miR-384 was reported to modulate tumor development *via* mediating target genes [36, 37]. The Rho-associated coiled-coil containing kinase 1 (ROCK1) gene is located on 18q11.1, and protein serine/threonine kinase encoded by the ROCK1 gene is activated after binding to the GTP-bound form of Rho [38]. ROCK1 has been reported to be involved in the pathogenesis of metabolism-related diseases, including hypertension, Alzheimer's disease, and diabetes [39, 40]. Previous studies have shown that ROCK1 has pivotal functions in LSCC. For example, high ROCK1 expression is positively correlated with LSCC tumor size and lymph node metastasis [40]. ROCK1 mediates epithelial-mesenchymal transition to promote LSCC metastasis *via* the JAK2/STAT3/ERK1/2 axis, and targeting ROCK1 might provide a potential therapeutic strategy for LSCC [41]. Crucially, ROCK1 is reported to be regulated by miRNAs, including miR-136-5p [42] and miR-195 [43]. Similarly, we observed that ROCK1 was raised in LSCC, miR-384 was negatively associated with ROCK1 in LSCC, and circHMGA2 was positively associated with ROCK1 expression. Furthermore, circHMGA2 modulated LSCC malignant phenotype *via* miR-384/ROCK1. Meanwhile, circHMGA2 knockdown reduced LSCC growth and inhibited M2 polarization *in vivo*.

Overall, this research explored the circHMGA2 function in LSCC and provided evidence that circHMGA2 acts as a novel oncogene in LSCC through the miR-384/ROCK1 axis, implying that circHMGA2 is an LSCC biomarker. However, this research had some limitations, as follows: (I) Only loss of function analysis was performed; (II) circHMGA2 might modulate LSCC through other mechanisms, which requires further investigation. We intend to perform further research to build upon these findings.

Funding

This research received no external funding.

Disclosures

The study was approved by the Bioethics Committee of the Second Affiliated Hospital of Nanchang University (Approval No. NO.YAN-2020-013).

The authors declare no conflict of interest.

References

1. Ouban A (2022): Filamin-A expression in laryngeal squamous cell carcinoma and its clinical significance. Histol Histopathol 37: 125-136.
2. de Carvalho GB, Kohler HF, Lira RB, et al. (2022): Survival results of 3786 patients with stage I or II laryngeal squamous cell carcinoma: a study based on a propensity score. Braz J Otorhinolaryngol 88: 337-344.
3. Cavaliere M, Bisogno A, Scarpa A, et al. (2021): Biomarkers of laryngeal squamous cell carcinoma: a review. Ann Diagn Pathol 54: 151787.
4. Wushouer A, Li W, Zhang M, et al. (2022): Comparison of treatment modalities for selected advanced laryngeal squamous cell carcinoma. Eur Arch Otorhinolaryngol 279: 361-371.
5. Ulshöfer CJ, Pfafenrot C, Bindereif A, et al. (2021): Methods to study circRNA-protein interactions. Methods 196: 36-46.
6. Costa MC, Calderon-Dominguez M, Mangas A, et al. (2021): Circulating circRNA as biomarkers for dilated cardiomyopathy etiology. J Mol Med (Berl) 99: 1711-1725.
7. Ma S, Gu X, Shen L, et al. (2021): CircHAS2 promotes the proliferation, migration, and invasion of gastric cancer cells by regulating PPM1E mediated by hsa-miR-944. Cell Death Dis 12: 863.

8. Meng S, Zhou H, Feng Z, et al. (2017): CircRNA: functions and properties of a novel potential biomarker for cancer. Mol Cancer 16: 94.
9. Zhang J, Li H, Li J, et al. (2022): CircRNA CORO1C regulates miR-654-3p/USP7 axis to mediate laryngeal squamous cell carcinoma progression. Biochem Genet 60: 1615-1629.
10. Guo Y, Huang Q, Zheng J, et al. (2020): Diagnostic role of dysregulated circular RNA hsa_circ_0036722 in laryngeal squamous cell carcinoma. Onco Targets Ther 13: 5709-5719.
11. Lu C, Shi X, Wang AY, et al. (2018): RNA-Seq profiling of circular RNAs in human laryngeal squamous cell carcinomas. Mol Cancer 17: 86.
12. Yu Z, Zhu X, Li Y, et al. (2021): Circ-HMGA2 (hsa_circ_0027446) promotes the metastasis and epithelial-mesenchymal transition of lung adenocarcinoma cells through the miR-1236-3p/ZEB1 axis. Cell Death Dis 12: 313.
13. Li S, Zhao J, Wen S, et al. (2023): CircRNA High Mobility Group At-hook 2 regulates cell proliferation, metastasis and glycolytic metabolism of nonsmall cell lung cancer by targeting miR-331-3p to upregulate High Mobility Group At-hook 2. Anticancer Drugs 34: 81-91.
14. Ma H, Li YN, Song L, et al. (2020): Macrophages inhibit adipogenic differentiation of adipose tissue derived mesenchymal stem/stromal cells by producing pro-inflammatory cytokines. Cell Biosci 10: 88.
15. Notararigo S, Varela E, Otal A, et al. (2022): Anti-inflammatory effect of an O-2-substituted (1-3)-β-D-glucan produced by Pediococcus parvulus 2.6 in a Caco-2 PMA-THP-1 co-culture model. Int J Mol Sci 23: 1527.
16. Wu T, Sun Y, Sun Z, et al. (2021): Hsa_circ_0042823 accelerates cancer progression via miR-877-5p/FOXM1 axis in laryngeal squamous cell carcinoma. Ann Med 53: 960-970.
17. Gao W, Guo H, Niu M, et al. (2020): circPARD3 drives malignant progression and chemoresistance of laryngeal squamous cell carcinoma by inhibiting autophagy through the PRKCI-Akt-mTOR pathway. Mol Cancer 19: 166.
18. Wu S, Huang X, Tie X, et al. (2021): Role and mechanism of action of circular RNA and laryngeal cancer. Pathol Res Pract 223: 153460.
19. Li R, Jiang J, Shi H, et al. (2020): CircRNA: a rising star in gastric cancer. Cell Mol Life Sci 77: 1661-1680.
20. Xue C, Li G, Lu J, et al. (2021): Crosstalk between circRNAs and the PI3K/AKT signaling pathway in cancer progression. Signal Transduct Target Ther 6: 400.
21. Zhao R, Li FQ, Tian LL, et al. (2019): Comprehensive analysis of the whole coding and non-coding RNA transcriptome expression profiles and construction of the circRNA-lncRNA co-regulated ceRNA network in laryngeal squamous cell carcinoma. Funct Integr Genomics 19: 109-121.
22. Han J, Lin Q, Dong C (2021): Plasma cell-free circRNAs panel act as fingerprint predicts the occurrence of laryngeal squamous cell carcinoma. Aging (Albany NY) 13: 17328-17336.
23. Lan J, Sun L, Xu F, et al. (2019): M2 macrophage-derived exosomes promote cell migration and invasion in colon cancer. Cancer Res 79: 146-158.
24. Mehla K, Singh PK (2019): Metabolic regulation of macrophage polarization in cancer. Trends Cancer 5: 822-834.
25. Yi B, Dai KJ, Yan ZQ, et al. (2022): Circular RNA PLCE1 promotes epithelial mesenchymal transformation, glycolysis in colorectal cancer and M2 polarization of tumor-associated macrophages. Bioengineered 13: 6243-6256.
26. McClellan JL, Steiner JL, Day SD, et al. (2014): Exercise effects on polyp burden and immune markers in the ApcMin/+ mouse model of intestinal tumorigenesis. Int J Oncol 45: 861-868.
27. Liu H, Yan S, Yang R, et al. (2024): Jiedu Xiaozheng Yin inhibits the progression of colitis associated colorectal cancer by stimulating macrophage polarization towards an M1 phenotype via the TLR4 pathway. Integr Cancer Ther 23: 15347354241247061.
28. Zhang M, Bai X, Zeng X, et al. (2021): circRNA-miRNA-mRNA in breast cancer. Clin Chim Acta 523: 120-130.
29. Chen P, Chen J, He L, et al. (2021): Identification of circRNA-miRNA-mRNA regulatory network in bladder cancer by integrated analysis. Urol Int 105: 705-715.
30. Lucas Grzelczyk W, Szemraj J, Kwiatkowska S, et al. (2019): Serum expression of selected miRNAs in patients with laryngeal squamous cell carcinoma (LSCC). Diagn Pathol 14: 49.
31. Luo M, Sun G, Sun JW (2019): MiR-196b affects the progression and prognosis of human LSCC through targeting PCDH-17. Auris Nasus Larynx 46: 583-592.
32. Wei Z, Chang K, Fan C (2019): Hsa_circ_0042666 inhibits proliferation and invasion via regulating miR-223/TGFBR3 axis in laryngeal squamous cell carcinoma. Biomed Pharmacother 119: 109365.
33. Yin X, Wang J, Shan C, et al. (2022): Circular RNA ZNF609 promotes laryngeal squamous cell carcinoma progression by upregulating epidermal growth factor receptor via sponging microRNA-134-5p. Bioengineered 13: 6929-6941.
34. Ma Q, Huai B, Liu Y, et al. (2021): Circular RNA circ_0020123 promotes non-small cell lung cancer progression through miR-384/TRIM44 Axis. Cancer Manag Res 13: 75-87.
35. Zhang Y, Tang Q, Huang XM, et al. (2020): Circular RNA circCNOT6L regulates cell development through modulating miR-384/FN1 axis in esophageal squamous cell carcinoma. Eur Rev Med Pharmacol Sci 24: 3674-3685.
36. Zhou W, She G, Yang K, et al. (2020): MiR-384 inhibits proliferation and migration of trophoblast cells via targeting PTBP3. Pregnancy Hypertens 21: 132-138.
37. Tan Y, Chen L, Li S, et al. (2020): MiR-384 inhibits malignant biological behavior such as proliferation and invasion of osteosarcoma by regulating IGFBP3. Technol Cancer Res Treat 19: 1533033820909125.
38. Rath N, Olson MF (2012): Rho-associated kinases in tumorigenesis: re-considering ROCK inhibition for cancer therapy. EMBO Rep 13: 900-908.
39. Hu YB, Zou Y, Huang Y, et al. (2016): ROCK1 is associated with Alzheimer's disease-specific plaques, as well as enhances autophagosome formation but not autophagic Aβ clearance. Front Cell Neurosci 10: 253.
40. Huyan T, Fan L, Zheng ZY, et al. (2024): ROCK1 inhibition improves wound healing in diabetes via RIPK4/AMPK pathway. Acta Pharmacol Sin 45: 1477-1491.
41. Yang L, Gong S, Qiao P, et al. (2023): CAFs-derived rho-associated kinase1 mediated EMT to promote laryngeal squamous cell carcinoma metastasis. Cancer Cell Int 23: 70.
42. Yang B, Zang J, Yuan W, et al. (2021): The miR-136-5p/ROCK1 axis suppresses invasion and migration, and enhances cisplatin sensitivity in head and neck cancer cells. Exp Ther Med 21: 317.
43. Liu Y, Liu J, Wang L, et al. (2017): MicroRNA-195 inhibits cell proliferation, migration and invasion in laryngeal squamous cell carcinoma by targeting ROCK1. Mol Med Rep 16: 7154-7162.